International Journal of Mass Spectrometry 306 (2011) 99–107

Contents lists available at ScienceDirect

International Journal of Mass Spectrometry

journal homepage: www.elsevier.com/locate/ijms

Amplified histidine effect in electron-transfer dissociation of histidine-rich peptides from histatin 5

Thomas W. Chung, František Tureček*

Department of Chemistry, Bagley Hall, Box 351700, University of Washington, Seattle, WA 98195-1700, USA

ARTICLE INFO

Article history:
Received 20 July 2010
Received in revised form 19 August 2010
Accepted 23 August 2010
Available online 31 August 2010

Keywords:
Electron-transfer dissociation
Histidine effect
Histatin 5
Histidine-rich tryptic peptide
Radical rearrangement
Zwitterion

ABSTRACT

We report electron-transfer dissociation (ETD) mass spectra of histidine-containing peptides DSHAK, FHEK, HHGYK, and HHSHR from trypsinolysis of histatin 5. ETD of both doubly and triply protonated peptides provided sequence ions of the *c* and *z* type. In addition, electron transfer to doubly protonated peptides produced abundant long-lived cation-radicals, $(M+2H)^{\bullet+}$, whose relative intensities depended on the peptide sequence and number of histidine residues. CID-MS^3 spectra of $(M+2H)^{\bullet+}$ cation-radicals were entirely different from the ETD spectra of the doubly charged ions and involved radical-driven losses of $C_4H_6N_2$ neutral fragments from the histidine residues and charge-driven backbone cleavages forming *b* and *y* ions. Product ions from CID of $(M+2H)^{\bullet+}$ were further characterized by CID-MS^4 spectra to distinguish the histidine residues undergoing loss of $C_4H_6N_2$. The ETD-CID-MS^n mass spectra are interpreted by considering radical-induced rearrangements of histidine side chains in the long-lived charge-reduced ions.

1. Introduction

Electron-transfer dissociation (ETD) [1] mass spectra of histidine-containing peptides have been reported to display interesting effects caused by specific reactions in the histidine side chain. Radicals formed by one-electron reduction of protonated imidazole ring in histidine residues undergo proton-catalyzed rearrangements that result in substantial stabilization of charge-reduced intermediates. This effect has been first observed by Xia et al. as "electron-transfer-no-dissociation" (ETnoD) and found to be specific for histidine-containing peptide ions [2]. We have studied the reaction mechanisms of what we called the *histidine effect* [3] for peptide ions ranging from singly protonated dipeptides (GH, HG) [4], tripeptides (HAL, AHL, ALH) [5], to several singly [6] and doubly protonated pentapeptides [3]. Charge reduction in singly protonated peptides forms neutral radicals that cannot be directly detected by mass spectrometry. However, peptide radicals can be reionized by collisions at keV kinetic energies to form cations, as in neutralization–reionization mass spectrometry [7,8], or anions, as in charge-reversal mass spectrometry [9,10], that provide information on the radical structure [6,11]. The rearrangements in histidine residues were found to be catalyzed by proton donors such as C-terminal and Asp carboxyl or N-terminal ammonium groups. The presumed mechanisms for the rearrangements [3–6] and their reactive intermediates are generically sketched in Scheme 1.

Upon electron attachment to the protonated His ring, the intermediate N-1′,N-3′-H-imidazolium radical [12] can undergo conformational rotations that bring the N-terminal ammonium or a carboxyl group to the proximity of the C-2′ atom which carries a substantial odd-electron density [5]. Proton transfer from the ammonium group to C-2′ (pathway a, Scheme 1) is highly exothermic and produces a stable cation-radical which is detected in the ETD spectrum [3]. Proton transfer from a carboxyl group is mildly exothermic to form a transient zwitterion consisting of the imidazoline cation-radical and the carboxylate anion (pathway b, Scheme 1) [5]. The zwitterion can undergo a further facile rearrangement by N-3′-H proton migration onto the carboxylate group to exothermically form an N-1′,C-2′-H radical. The latter is more stable than the initial histidine radical and can be detected in the ETD spectrum. Upon collisional excitation, the rearranged His radical can eliminate the $C_4H_6N_2$ side-chain fragment, converting the His residue to a Gly C_α radical. The exact structure of the neutral $C_4H_6N_2$ fragment is unknown but most likely corresponds to a methylimidazole tautomer or a mixture thereof.

Experimental evidence for the histidine rearrangement followed from charge-reversal ($^+CR^-$) mass spectra of singly protonated peptides and collision induced dissociation (CID-MS^3) spectra of charge-reduced but non-dissociating peptide ions. The ETD-CID-MS^3 spectra showed that long-lived charge-reduced peptide cation-radicals did not undergo backbone N–C_α bond cleavages which are typical for ETD. Instead, CID of charge-reduced ions

* Corresponding author. Tel.: +1 206 685 2041; fax: +1 206 685 3478.
E-mail address: turecek@chem.washington.edu (F. Tureček).

1387-3806/$ – see front matter © 2010 Elsevier B.V. All rights reserved.
doi:10.1016/j.ijms.2010.08.021

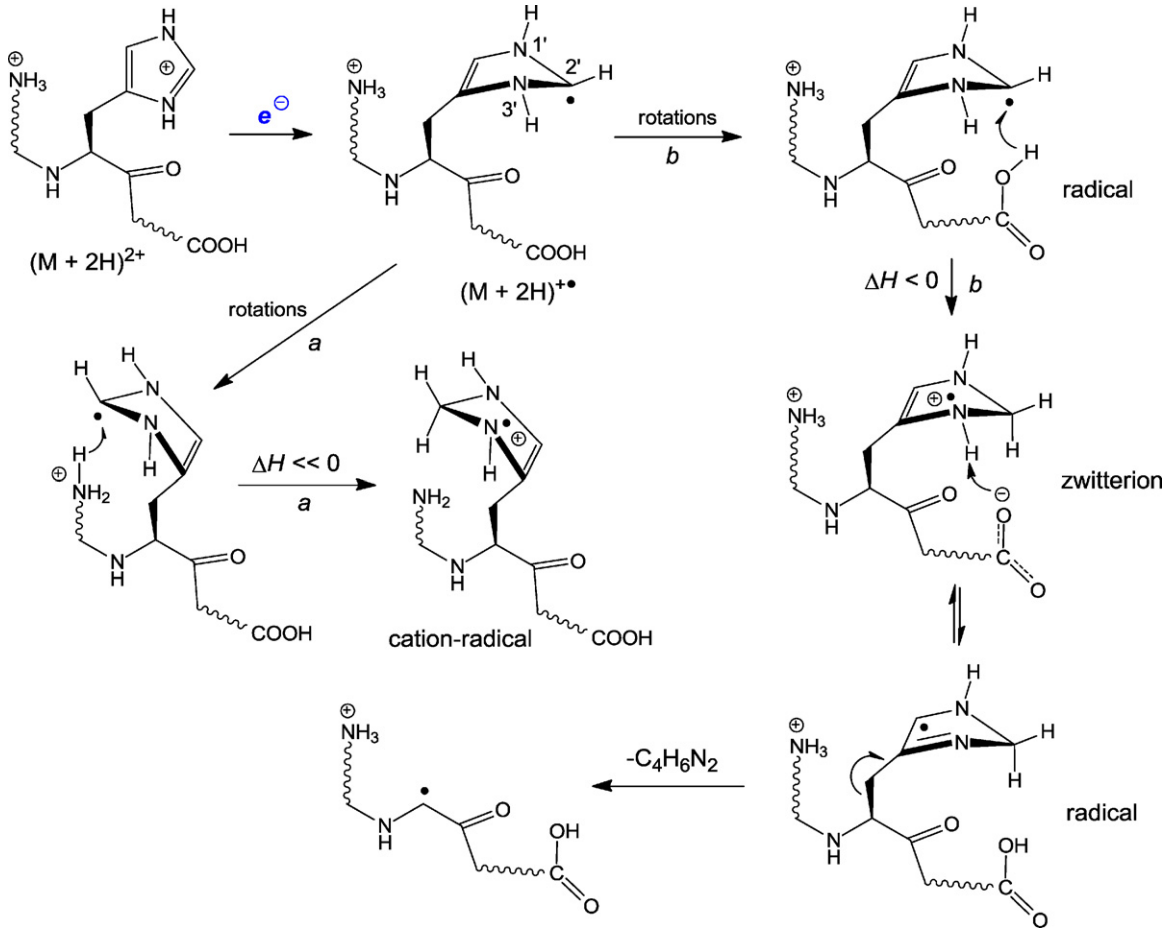

Scheme 1.

resulted in the loss of a $C_4H_6N_2$ neutral fragment from the histidine side chain that was indicative of a rearrangement [5]. Since the previous research on histidine-containing peptides concerned only synthetic model compounds, it became of interest to investigate peptides produced from natural sources, such as histidine-containing peptides and proteins. A convenient source is found among histidine-rich antibacterial proteins of the histatin family [13]. Histatins 1, 3, and 5 are small cationic proteins containing, respectively, 38, 32, and 24 amino acid residues. They are secreted by human parotid and mandibular glands and are present in saliva where they have several protective functions [14]. Histatin 5 has the sequence DSHAKRHHGYKRKFHEKHHSHRGY which is a convenient source of histidine-containing peptides upon trypsinolysis, e.g., DSHAK, HHGYK, FHEK, and HHSHR. These small (4–5 residues) basic peptides thus have naturally different numbers and positions of His residues that can be expected to produce doubly and triply charged ions by electrospray and thus be favorable for studying the histidine effect. We now report an experimental ETD-CID-MS^n study focused on the dissociations induced by electron transfer and the analysis of charged-reduced intermediates. We wish to show that the histidine effect is amplified in the presence of multiple histidine residues in a fashion which is also sequence dependent.

2. Experimental

2.1. Materials and methods

Histatin 5 protein (98% pure) was purchased from Aroz Technologies (Cincinnati, OH, USA). Histatin 5 was subjected to proteolysis using immobilized trypsin (Catalog No. V9013, Promega Corp., Madison, WI, USA), as described by the manufacturer. Briefly, 3.0 mg of histatin 5 was first sonicated in 100 μL of >18.2 Ω MilliQ water to make a 30 mg/mL protein stock solution. A so-called "protein digestion mixture" was prepared by combining in a 2.0 mL microcentrifuge tube 16.7 μL of 30 mg/mL histatin 5 protein stock solution, 48 μL acetonitrile, and 55.3 μL of 50 mM ammonium bicarbonate buffer. Immobilized trypsin, which comes conjugated to a cellulose resin and is provided in a 1:1 (v/v) slurry in 50 mM CH_3CO_2H, 1 mM $CaCl_2$, and 0.02% NaN_3, was resuspended and 600 μL of it was dispensed onto a spin column, which was then centrifuged to remove liquid from the resin. The resin was washed with 400 μL of 50 mM ammonium bicarbonate. This wash cycle was repeated for a total of three times. The protein digestion mixture was added quantitatively and directly to the resin in the spin basket and incubated at room temperature for 30 min. Peptide recovery was performed by adding 300 μL of "Peptide Recovery Buffer" to the spin column and briefly centrifuging to remove the peptide solution from the resin and into a clean 2 mL microcentrifuge tube. This "Peptide Recovery Buffer" was previously prepared by combining 400 μL acetonitrile, 20 μL of 10% trifluoroacetic acid, and 580 μL of >18.2 Ω MilliQ water. The peptide recovery step was repeated in order to achieve a final tryptic peptide solution of no more than 720 μL for downstream applications. A sample solution was prepared by combining 371.5 μL of the tryptic peptide solution with 1.3285 mL of a 50/50 methanol–water solution that encompassed 2% acetic acid. Direct infusion electrospray of this single, heterogeneous sample solution afforded multiply charged peptide ions DSHAK, HHGYK, FHEK, and HHSHR.

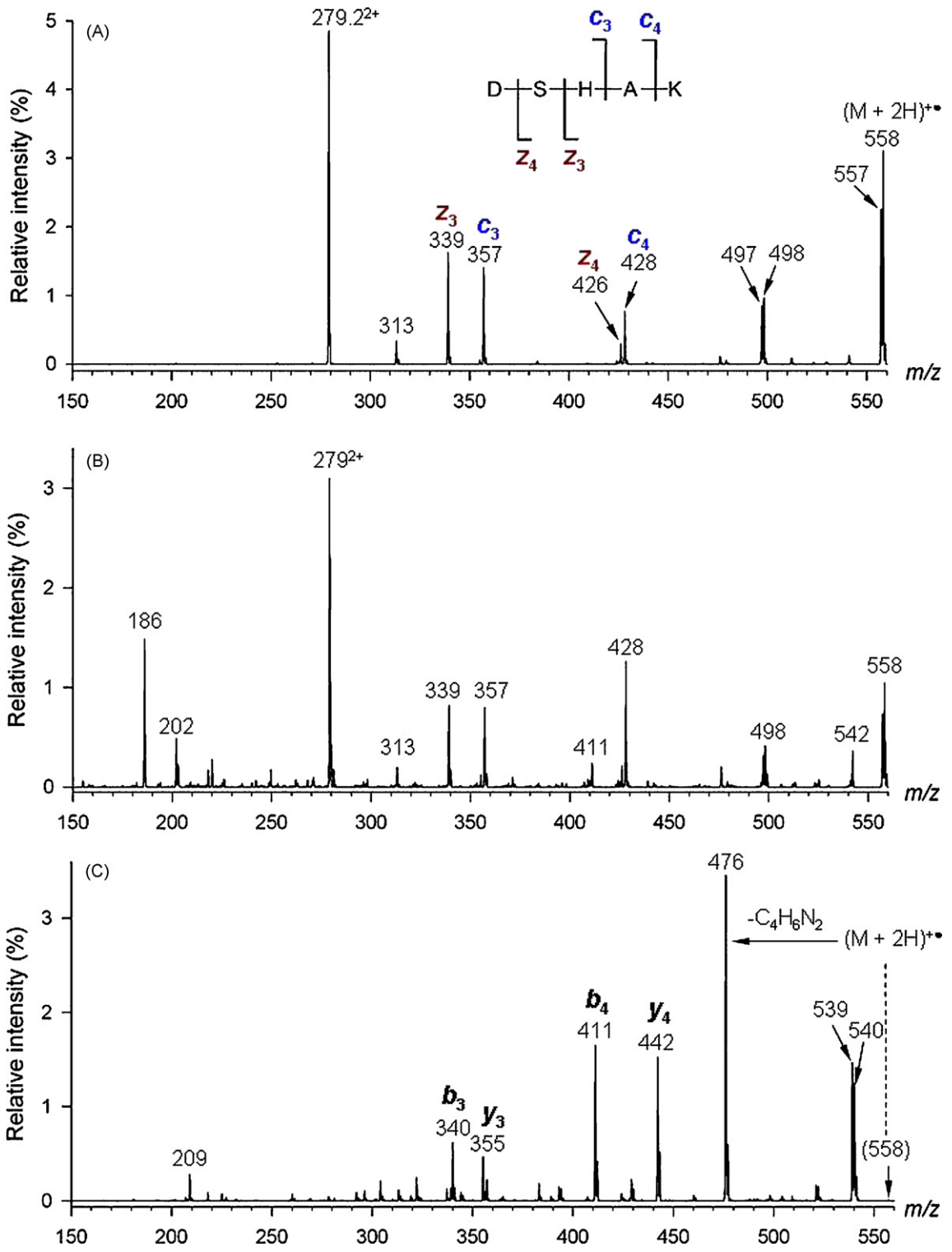

Fig. 1. ETD mass spectra of (A) $(DSHAK+2H)^{2+}$ (m/z 279.2) and (B) $(DSHAK+3H)^{3+}$ (m/z 186.4) ions. (C) CID-MS^3 mass spectrum of mass selected $(DSHAK+2H)^{\bullet+}$ (m/z 558) from charge-reduction of $(DSHAK+2H)^{2+}$. The ion relative intensities were normalized to the sum of intensities of all charge-reduced ions but excluding the residual precursor ion intensity.

Electron-transfer dissociation mass spectra were measured on a Thermo Fisher Scientific (San Jose, CA, USA) LTQ XL linear ion trap instrument outfitted with a chemical ionization source for the production of fluoranthene anion radicals as ETD reagent. Precursor cations $(M+2H)^{2+}$ and $(M+3H)^{3+}$ were mass isolated with a window of 1.6–2.5 and 0.7–2.0 m/z units, respectively, to accommodate nearest ^{13}C isotopologues and allowed to react for 100, 200, and 300 ms with fluoranthene anions. The 200 ms ETD spectra are reported.

Survivor charge-reduced $(M+2H)^{\bullet+}$ from electron transfer were mass selected with a 1 m/z unit window and collisionally dissociated (CID-MS^3) with the ion excitation energy set at 20% on the instrument scale. This gave abundant $(M+2H-C_4H_6N_2)^{\bullet+}$ ions, which were subsequently mass selected and subjected to collisional

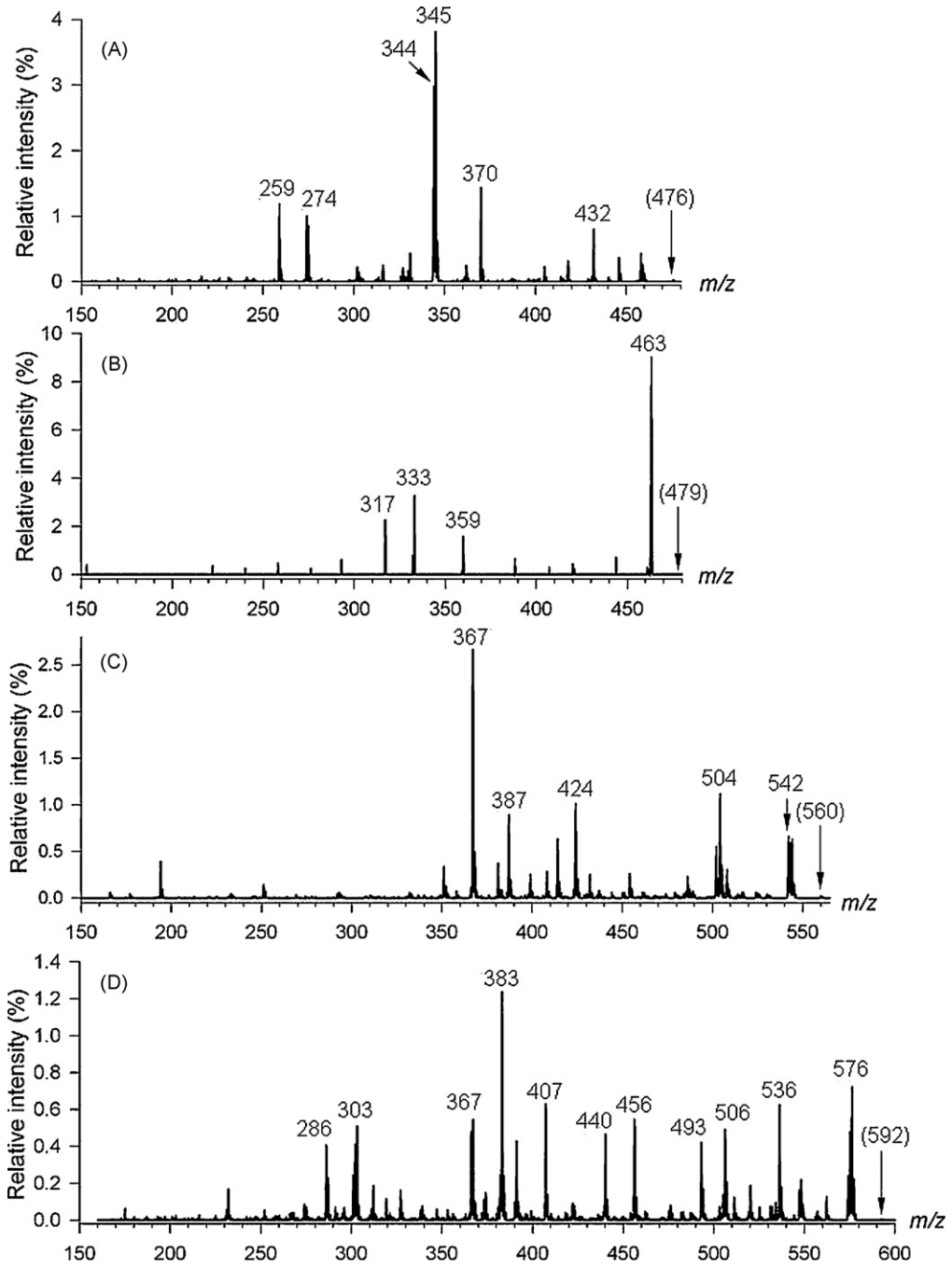

Fig. 2. CID-MS^4 mass spectra of (A) m/z 476 ion by loss of $C_4H_6N_2$ from charge-reduced (DSHAK+2H)$^{\bullet+}$; (B) m/z 479 ion by loss of $C_4H_6N_2$ from charge-reduced (FHEK+2H)$^{\bullet+}$; (C) m/z 560 ion by loss of $C_4H_6N_2$ from charge-reduced (HHGYK+2H)$^{\bullet+}$, and (D) m/z 592 ion by loss of $C_4H_6N_2$ from charge-reduced (HHSHR+2H)$^{\bullet+}$. The ion relative intensities were normalized to the sum of intensities of all charge-reduced ions.

activation with the ion excitation energy set at 20% on the instrument scale to yield the CID-MS^4 spectra reported here. CID-MS^3 mass spectra were also taken of all ETD *c* and *z* sequence fragments.

3. Results

3.1. DSHAK

The DSHAK peptide formed singly, doubly and triply charged ions by electrospray that appeared at m/z 557.3 (48%), m/z 279.1 (48%) and m/z 186.4 (4%), respectively. Thus only about a half of the produced ion population was useful for ETD. Electron transfer to the m/z 279.1 precursor ion resulted in the formation of an abundant

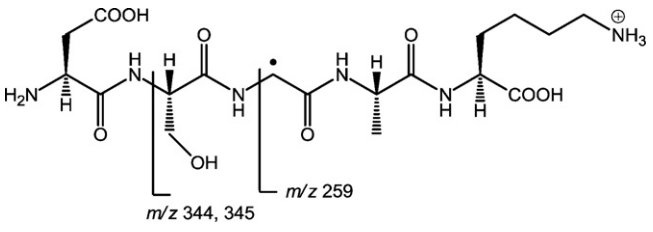

Scheme 2.

charge-reduced $(M+2H)^{\bullet+}$ cation-radical at m/z 558, which constituted 26% of the sum of charge-reduced ion intensities (Fig. 1A). Fragmentation proceeded by loss of H (m/z 557), $C_2H_4O_2$ (m/z 498), and by backbone cleavages forming the c_4 (m/z 428), z_4 (m/z 426), c_3 (m/z 357) and z_3 (m/z 339) ions. The ETD mass spectrum of the triply protonated ion (m/z 186.4) displayed similar fragments (Fig. 1B). In particular, the singly charged backbone ions c_4, z_4, c_3, and z_3 were formed together with the $(M+2H)^{\bullet+}$ cation-radical. In contrast, the presence in the spectrum of the singly reduced $(M+3H)^{\bullet 2+}$ ion cannot be confirmed because of overlap with the ^{13}C isotope satellite of the $(M+2H)^{2+}$ ion at m/z 280. As a general remark, the ETD mass spectrum of the $(M+3H)^{3+}$ ion shows more secondary fragments (m/z 411, 371, 250, 220, 202, 186, etc.) presumably due to greater ion excitation by electron transfer to the triply charged ion compared to the same process concerning the doubly charged ion. The origin of these singly charged secondary fragments has been established by ETD-MS^3 experiments where each of the primary c and z fragments from ETD was mass selected and collisionally dissociated. For example, CID of the c_4 fragment ion (m/z 428) produced the m/z 411 ion as a dominant secondary fragment by loss of ammonia. We note that although the m/z 411 ion formally corresponds to a b_4 sequence ion, its formation through the c_4 ion is corroborated by the ETD-MS^3 spectrum. Likewise, the m/z 202 ion in the Fig. 1B spectrum, which formally is a z_2(AK) fragment, is a dominant secondary fragment from CID of the z_4 ion at m/z 426 and presumably is formed by a cascade elimination [15] of a neutral

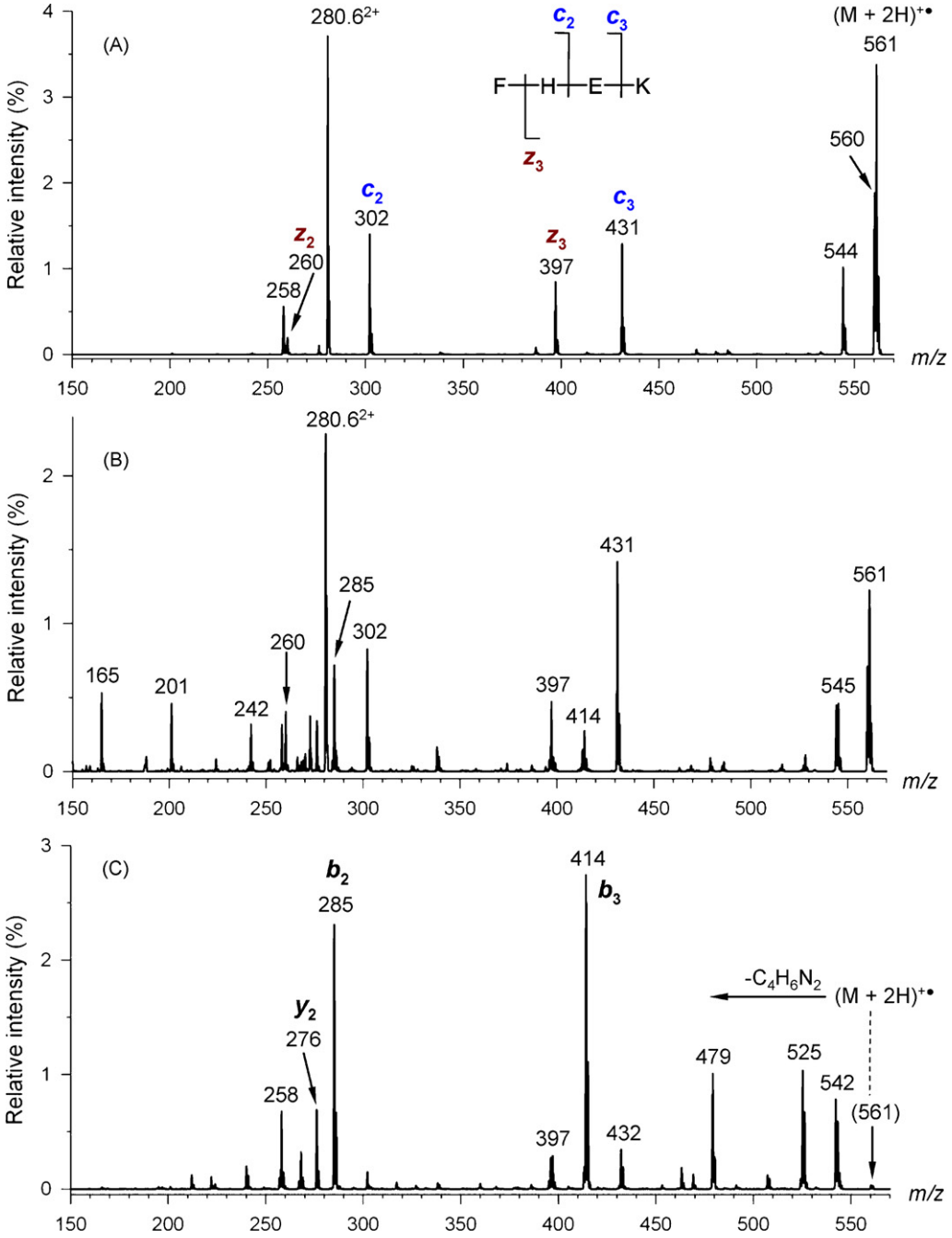

Fig. 3. ETD mass spectra of (A) $(FHEK+2H)^{2+}$ (m/z 280.6) and (B) $(FHEK+3H)^{3+}$ (m/z 187.4) ions. (C) CID-MS^3 mass spectrum of mass selected $(FHEK+2H)^{\bullet+}$ (m/z 561) from charge-reduction of $(FHEK+2H)^{2+}$. The ion relative intensities were normalized to the sum of intensities of all charge-reduced ions but excluding the residual precursor ion intensity.

fragment containing the deaminated serine and histidine residue ($HOCH_2CHCONHCH(CH_2C_3H_3N_2)CONH$). Interestingly, the formation of the m/z 202 from the z_3 ion (m/z 339) is much weaker, the main dissociation being an elimination of a C_3H_8N radical from the Lys residue.

The efficiency for ET (%E) to the doubly and triply charged peptide ions was 77% and 92%, respectively, when expressed as a ratio of the sum of all charge-reduced ion intensities, ΣI_{ETD}, to the total ion count, $\Sigma I_{ETD} + I_P$, including the residual precursor ion intensity I_P (Eq. (1)). Both these efficiencies refer to 200 ms ion–ion interaction time.

$$\%E = \frac{100 \sum I_{ETD}}{I_P + \sum I_{ETD}} \quad (1)$$

The charge-reduced $(M+2H)^{\bullet+}$ cation-radicals from ETD of m/z 279.1 and m/z 186.4 gave very similar CID-MS^3 spectra as represented by that from m/z 279.1 (Fig. 1C). The ETD-CID-MS^3 spectrum is dominated by a fragment ion at m/z 476 by loss of a 82 Da neutral fragment, presumably $C_4H_6N_2$ from the His side chain [2,16]. A conspicuous feature of Fig. 1C spectrum is the absence or very low intensity of the c_4, z_4, c_3, and z_3 backbone fragment ions (cf. Fig. 1A). Backbone dissociations are represented by abundant y_4, b_4, y_3, and b_3 ions at m/z 442, 411, 355, and 340, respectively. These charge-induced dissociations compete with the elimination of the His $C_4H_6N_2$ side-chain fragment. The pertinent fragment ion at m/z 476 was further selected by mass and analyzed by CID. The CID-MS^4 spectrum (Fig. 2A) showed eliminations of peripheral groups (CO_2, H_2O, CH_2O) in combination with backbone dissociations by eliminations of amino acid residues from the N-terminus, e.g., ($AspNH_2$–H) (m/z 345), $AspNH_2$ (m/z 344), and ($AspSerNH_2$–H) (m/z 259). These dissociations must involve N–C_α bond cleavages which may be triggered by radical migrations along the backbone and side chains in the m/z 476 cation-radical [17]. The backbone cleavages are sketched in Scheme 2, although the exact mechanisms have not been established.

3.2. FHEK

Electrospray of the FHEK peptide produced singly, doubly, and triply charged ions at m/z 560.3 (35%), m/z 280.6 (57%), and m/z 187.4 (8%), respectively. The ETD spectra of the doubly and triply charged ions were analogous to those of DSHAK ions. The ETD mass spectrum of the major doubly charged ion at m/z 280.6 gave an abundant charge-reduced $(M+2H)^{\bullet+}$ cation-radical at m/z 561 which comprised 34% of the sum of charge-reduced ion intensities (Fig. 3A). Backbone fragment ions appeared at m/z 431 (c_3), 397 (z_3), 302 (c_2) and a weak peak at m/z 260 (z_2). The abundant backbone fragment ions all contained the His residue. The ETD mass spectrum of the triply charged ion (m/z 187.4) also gave the singly charged c and z fragment ions, in addition to numerous fragments from consecutive dissociations (Fig. 3B). The electron-transfer efficiency at 200 ms ion–ion interaction time was %E = 80% and 85% for the doubly and triply charged precursor ions, respectively. CID-MS^3 of the charge-reduced $(M+2H)^{\bullet+}$ ion at m/z 561 resulted in losses of water, ammonia, and backbone cleavages forming the b_3 (m/z 414), b_2 (m/z 285) and y_2 (m/z 276) fragment ions (Fig. 3C). Loss of $C_4H_6N_2$ was also observed (m/z 479), although at lower relative abundance than for DSHAK. CID-MS^4 of the m/z 479 ion resulted in a dominant loss of a 16 Da neutral fragment, presumably NH_2, to give a m/z 463 fragment ion (Fig. 2B). This somewhat unusual dissociation can be facilitated by migration of a benzylic H-atom from the Phe residue [17] to the His C_α radical which requires a six-membered transition state [18] and activates the N-terminal H_2N–C bond for homolytic dissociation (Scheme 3).

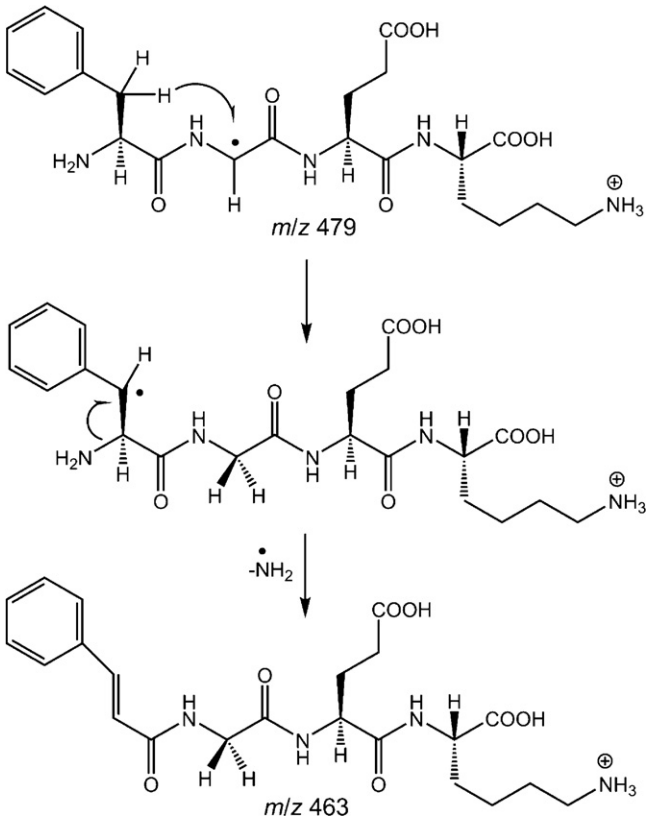

Scheme 3.

3.3. HHGYK

Electrospray of the HHGYK peptide produced singly, doubly and triply charged ions at m/z 641.4 (32%), m/z 321.2 (28%) and m/z 214.1 (40%), respectively. ETD of the doubly and triply charged HHGYK ions proceeded with %E = 90 and 99%, respectively, at 200 ms ion–ion interaction time. ETD of the doubly charged ion at m/z 321.2 produced a dominant charge-reduced $(M+2H)^{\bullet+}$ ion at m/z 642 that constituted 44% of total ETD ion intensities. A series of backbone c fragments were found at m/z 292 (c_2), 349 (c_3), and 512 (c_4), which were complemented by the z_4 ion at m/z 488 (Fig. 4A). ETD of the triply charged ion at m/z 214.1 gave an abundant $(M+2H)^{\bullet+}$ ion at m/z 642 and a number of fragments due to backbone and consecutive dissociations (Fig. 4B). CID-MS^3 of the $(M+2H)^{\bullet+}$ ion at m/z 642 showed a dominant loss of $C_4H_6N_2$ (m/z 560, Fig. 4C). The other dissociations consisted of sequential eliminations of water and ammonia combined with loss of H-atoms to give fragment ion clusters at m/z 623–626 and m/z 605–608. Backbone dissociations were represented by the abundant b_2 fragment ion at m/z 275.

CID-MS^4 of the m/z 560 ion due to loss of $C_4H_6N_2$ formed a dominant m/z 367 fragment ion which corresponds to a y_3(GYK) ion (Fig. 2C). In addition, the spectrum displayed a regular y_4(HGYK) sequence fragment ion at m/z 504, as well as a modified y_4(GGYK) ion at m/z 424. The m/z 504 fragment ion can be expected from a m/z 560 precursor that lost the side chain from the N-terminal His_1 residue, while the m/z 424 fragment ion must be formed from a precursor that lost the side chain from the internal His_2 residue. Hence, the CID-MS^4 spectrum indicates that the loss of the His side chain was non-specific as to the His residue position in the peptide sequence.

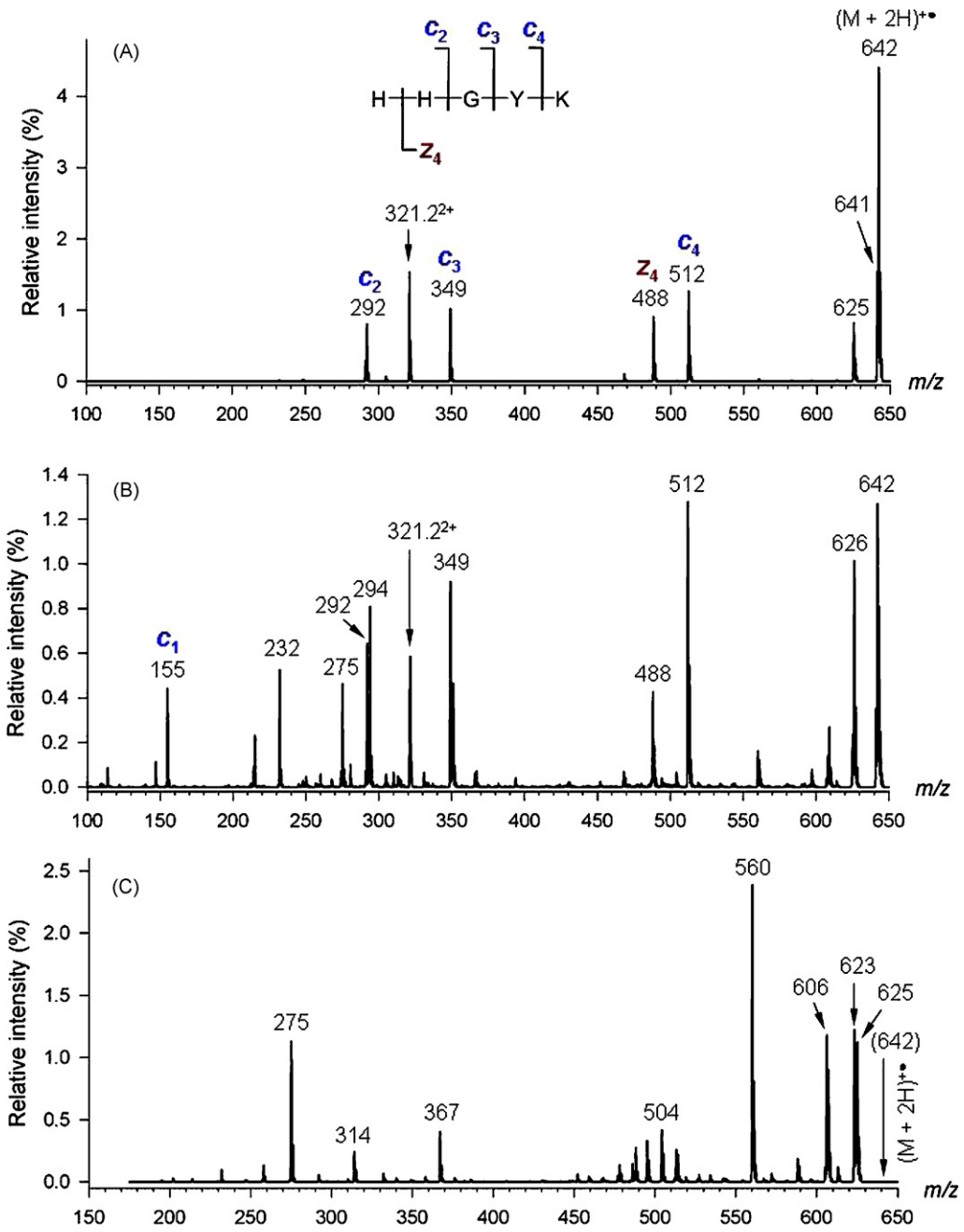

Fig. 4. ETD mass spectra of (A) $(HHGYK+2H)^{2+}$ (m/z 321.2) and (B) $(HHGYK+3H)^{3+}$ (m/z 214.1) ions. (C) CID-MS^3 mass spectrum of mass selected $(HHGYK+2H)^{\bullet+}$ (m/z 642) from charge-reduction of $(HHGYK+2H)^{2+}$. The ion relative intensities were normalized to the sum of intensities of all charge-reduced ions but excluding the residual precursor ion intensity.

3.4. HHSHR

This last tryptic peptide contained three His residues and formed singly, doubly and triply charged ions upon electrospray that appeared at m/z 673.4 (18%), m/z 337.2 (30%), and m/z 224.9 (51%), respectively, giving >80% of ion precursors suitable for ETD. Electron transfer to the doubly charged ion at m/z 337.2 was 91% efficient and gave an intense charge-reduced $(M+2H)^{\bullet+}$ ion at m/z 674 that constituted 52% of charge-reduced ion intensities (Fig. 5A). ETD of the triply charged ion at m/z 224.8 was 99% efficient at 200 ms of ion–ion interaction time. Interestingly, the charge-reduced ion from the m/z 224.8 precursor appeared at m/z 675 and must have corresponded to $(M+3H)^+$ (Fig. 5B). The CID-MS^3 mass spectra of the $(M+2H)^{\bullet+}$ and $(M+3H)^+$ ions were distinctly different in that the former showed a dominant loss of $C_4H_6N_2$ to give a m/z 592 fragment (Fig. 5C), while the latter involved a dominant loss of ammonia to give a m/z 658 fragment (Fig. 5D). These dissociations are consistent with the radical nature of the $(M+2H)^{\bullet+}$ ion to undergo a radical-induced loss of the His side chain on the one hand, and the closed-shell nature of the $(M+3H)^+$ ion to eliminate ammonia via a charge-driven reaction on the other.

CID-MS^4 of the m/z 592 ion gave several products (Fig. 2D). Among those, the m/z 536 ion can be formed by loss of a 56 Da fragment from the truncated N-terminal His_1 residue. Likewise, the m/z 383 fragment ion can correspond to a z_3 ion, indicating the His_4 residue was intact. We did not attempt to assign the other fragments in the Fig. 5D spectrum.

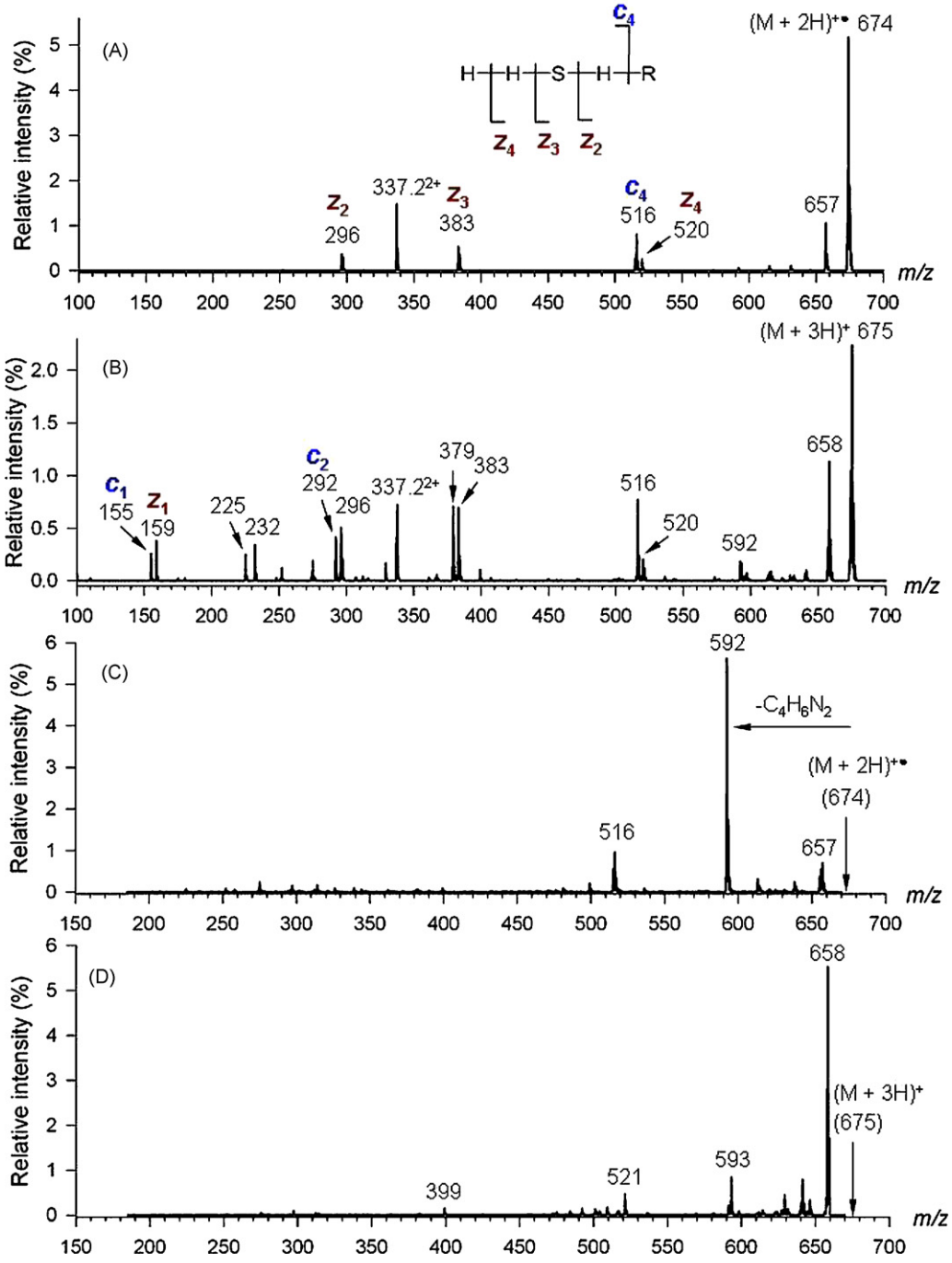

Fig. 5. ETD mass spectra of (A) $(HHSHR+2H)^{2+}$ (m/z 337.2) and (B) $(HHSHR+3H)^{3+}$ (m/z 224.8) ions. (C) CID-MS^3 mass spectrum of mass selected $(HHSHR+2H)^{\bullet+}$ (m/z 674) from charge-reduction of $(HHSHR+2H)^{2+}$. (D) CID-MS^3 mass spectrum of mass selected $(HHSHR+3H)^{+}$ (m/z 675) from charge-reduction of $(HHSHR+3H)^{3+}$. The ion relative intensities were normalized to the sum of intensities of all charge-reduced ions but excluding the residual precursor ion intensity.

4. Discussion

The above-presented data indicate that His residues have specific effects on ETD spectra of ions from small tryptic peptides. First, the electron-transfer efficiency weakly correlated with the number of His residues in the peptide ion, whereby $\%E = 77$, 80, 90, and 91% for doubly protonated DSHAK, FHEK, HHGYK, and HHSHR, respectively. A stronger effect was found for the relative intensities of charge-reduced, non-dissociating, $(M+2H)^{\bullet+}$ cation-radicals which increased from 26% for doubly protonated DSHAK to 34% for FHEK, 44% for HHGYK, and 52% for HHSHR. The combined relative intensities of c and z backbone fragments from ETD were practically identical (31%) for the three Lys-terminated peptides, although their distribution differed. All c and z ions from the Lys-containing peptides contained protonated His residues, whereas the complementary Lys-containing fragments were neutral. The increased $(M+2H)^{\bullet+}$ relative intensities in the ETD spectra of FHEK and HHGYK were presumably due to decreased side-chain dissociations by loss of ammonia or $C_2H_4O_2$ from the Asp residue. The Arg-terminated peptide showed lower $c+z$ relative abundances (21%). In addition, the z_2 and z_3 fragments from HHSHR showed substantial $(z+1)$ satellites, and the c_4 ion was accompanied by a (c_4-1) ion. These were due to intramolecular H-atom migrations occurring in ion–molecule com-

plexes of complementary *c* and *z* fragments, as studied previously [19].

CID of long-lived $(M+2H)^{\bullet+}$ cation-radicals showed radical-induced losses of $C_4H_6N_2$ fragments from the His residues, which competed with proton-driven losses of water, ammonia, and backbone dissociations forming *b* and *y* fragment ions. The loss of $C_4H_6N_2$ upon CID is thought to originate from rearranged $(M+2H)^{\bullet+}$ charge-reduced ions according to Scheme 1 [3–6] and the extent of this fragmentation can presumably be taken as a marker for the population of rearranged ions. The rearrangement occurs in the imidazole ring, requires an internal catalysis by a proton donor, and results in a stabilization of the charge-reduced ion [3–6]. The tryptic peptides from histatin 5 contain basic residues at the C-terminus and 1–3 histidine residues. In keeping with previous studies of histidine-containing peptide ions, we presume that the doubly charged ions are protonated at the C-terminal basic amino acid (Lys or Arg) and at one of the His residues. In charge-reduced $(DHSAK+2H)^{\bullet+}$, the His rearrangement can be catalyzed by the Asp or C-terminal COOH groups; accordingly, the loss of $C_4H_6N_2$ is a dominant fragmentation channel. In contrast, charge-reduced $(FHEK+2H)^{\bullet+}$ shows less abundant loss of $C_4H_6N_2$ which we interpret as less efficient histidine rearrangement due to a lower accessibility to the COOH group.

Increasing the number of His residues in $(HHGYK+2H)^{\bullet+}$ and $(HHSHR+2H)^{\bullet+}$ promotes the loss of $C_4H_6N_2$. The backbone fragmentations upon CID-MS^4 of the *m*/*z* 560 ion from HHGYK then suggest that the loss of $C_4H_6N_2$ had occurred from either His residue. This indicates a statistical effect whereby either His residue is protonated in the precursor ions and then undergoes a rearrangement in the charge-reduced ion. We also note that charge-reduced peptide ions that lack histidine residues undergo different dissociations, as studied recently [20].

5. Conclusions

Histidine-rich tryptic peptides from histatin 5 form abundant charge-reduced, non-dissociating cation-radicals upon electron transfer. CID of the charge-reduced ions triggers elimination of $C_4H_6N_2$ which depends on the peptide sequence and is amplified in peptide ions containing two or three His residues. This amplified histidine effect is interpreted by facile internal rearrangement in His radicals to form intermediates which are prone for the $C_4H_6N_2$ elimination.

Acknowledgements

Thanks are due to Dr. Priska von Haller of the University of Washington Proteomics Resource Center for access to the Thermo LTQ XL instrument. Research support by the NSF (Grant CHE-0750048) is gratefully appreciated.

References

[1] J.E.P. Syka, J.J. Coon, M.J. Schroeder, J. Shabanowitz, D.F. Hunt, Proc. Natl. Acad. Sci. U.S.A. 101 (2004) 9528.
[2] Y. Xia, H.P. Gunawardena, D.E. Erickson, S.A. McLuckey, J. Am. Chem. Soc. 129 (2007) 12232.
[3] F. Tureček, T.W. Chung, C.L. Moss, J.A. Wyer, A. Ehlerding, H. Zettergren, S.B. Nielsen, P. Hvelplund, J. Chamot-Rooke, B. Bythell, B. Paizs, J. Am. Chem. Soc. 132 (2010) 10728.
[4] F. Tureček, C. Yao, Y.M.E. Fung, S. Hayakawa, M. Hashimoto, H. Matsubara, J. Phys. Chem. B 113 (2009) 7347.
[5] F. Turecek, J.W. Jones, T. Towle, S. Panja, S.B. Nielsen, P. Hvelplund, B. Paizs, J. Am. Chem. Soc. 130 (2008) 14584.
[6] F. Tureček, S. Panja, J.A. Wyer, A. Ehlerding, H. Zettergen, S.B. Nielsen, P. Hvelplund, B. Bythell, B. Paizs, J. Am. Chem. Soc. 131 (2009) 16472.
[7] (a) P.M. Curtis, B.W. Williams, R.F. Porter, Chem. Phys. Lett. 65 (1979) 296;
(b) P.C. Burgers, J.L. Holmes, A.A. Mommers, J.K. Terlouw, Chem. Phys. Lett. 102 (1983) 1;
(c) P.O. Danis, C. Wesdemiotis, F.W. McLafferty, J. Am. Chem. Soc. 105 (1983) 7454.
[8] For recent reviews see;;
(a) F. Turecek, Top. Curr. Chem. 225 (2003) 77;
(b) D.V. Zagorevskii, in: J.A. McCleverty, T.J. Meyer (Eds.), Comprehensive Coordination Chemistry II, Elsevier, Oxford, 2004, p. 381;
(c) F. Turecek, in: P.B. Armentrout (Ed.), Encyclopedia of Mass Spectrometry, vol. 1, Elsevier, Amsterdam, 2003, p. 528 (Chapter 7);
(d) D.V. Zagorevskii, Coord. Chem. Rev. 225 (2002) 5;
(e) P. Gerbaux, C. Wentrup, R. Flammang, Mass Spectrom. Rev. 19 (2000) 367;
(f) D.V. Zagorevskii, J.L. Holmes, Mass Spectrom. Rev. 18 (1999) 87;
(g) C. Schalley, G. Hornung, D. Schröder, H. Schwarz, Chem. Soc. Rev. 27 (1998) 91.
[9] D. Schröder, in: P.B. Armentrout (Ed.), Encyclopedia of Mass Spectrometry, vol. 1, Elsevier, Amsterdam, 2004, pp. 521–528 (Chapter 8).
[10] S. Hayakawa, J. Mass Spectrom. 39 (2004) 111.
[11] P. Hvelplund, B. Liu, S.B. Nielsen, S. Panja, J.C. Poully, K. Støchkel, Int. J. Mass Spectrom. 263 (2007) 66.
[12] V.Q. Nguyen, F. Turecek, J. Mass Spectrom. 31 (1996) 1173.
[13] F.G. Oppenheim, T. Xu, F.M. McMillian, S.M. Levitz, R.D. Diamond, G.D. Offner, R.F. Troxler, J. Biol. Chem. 263 (1988) 7472.
[14] E.J. Helmerhorst, R.F. Troxler, F.G. Oppenheim, Proc. Natl. Acad. Sci. U.S.A. 98 (2001) 14637.
[15] N. Leymarie, C.E. Costello, P.B. O'Connor, J. Am. Chem. Soc. 125 (2003) 8949.
[16] Y.M.E. Fung, T.-W.D. Chan, J. Am. Soc. Mass Spectrom. 16 (2005) 1523.
[17] (a) T. Ly, R.R. Julian, J. Am. Soc. Mass Spectrom. 20 (2009) 1148;
(b) Q. Sun, H. Nelson, T. Ly, B.M. Stoltz, R.R. Julian, J. Proteome Res. 8 (2009) 958.
[18] T.W. Chung, F. Tureček, J. Am. Soc. Mass Spectrom. 21 (2010) 1279.
[19] (a) C. Lin, P.B. O'Connor, J.J. Cournoyer, J. Am. Soc. Mass Spectrom. 17 (2006) 1605;
(b) P.B. O'Connor, C. Lin, J.J. Cournoyer, J.L. Pittman, M. Belyayev, B.A. Budnik, J. Am. Soc. Mass Spectrom. 17 (2006) 576;
(c) R.A. Zubarev, D.M. Horn, E.K. Fridriksson, N.L. Kelleher, N.A. Kruger, M.A. Lewis, B.K. Carpeneter, F.W. McLafferty, Anal. Chem. 72 (2000) 563.
[20] H. Ben Hamidane, D. Chiappe, R. Hartmer, A. Vorobyev, M. Moniatte, Y.O. Tsybin, J. Am. Soc. Mass Spectrom. 20 (2009) 567.